Iranian Journal of Hydrogen & Fuel Cell 2(2016) 137-149

Iranian Journal of Hydrogen & Fuel Cell

IJHFC

Journal homepage://ijhfc.irost.ir

Effects of coating thickness on corrosion and contact resistance behavior of TiN coated AISI 316L as bipolar plates for PEMFC

A. Hedayati[1,2], S. Asghari[2,*], A.H. Alinoori[2], M. Koosha[2], E. Vuorinen[1]

[1] Department of Engineering Sciences and Mathematics, Luleå University of Technologies 97187 Luleå, Sweden
[2] Institute of Materials and Energy, Iranian Space Research Center, 7th kilometer of Imam Khomeini ave., Isfahan, Iran

Article Information

Article History:

Received:
16 Oct 2016
Received in revised form:
14 Nov 2016
Accepted:
15 Nov 2016

Keywords

Proton Exchange Membrane-Fuel Cells
AISI 316L Stainless Steel Bipolar Plates
PVD Coating
Titanium Nitride (TiN) Coating

Abstract

In the polymer electrolyte membrane fuel cells (PEMFCs), low corrosion resistance and high interfacial contact resistance (ICR) are two controversial issues in usage of AISI 316L stainless steel as a metallic bipolar plate. For solving these problems, investigation and development of different coatings and/or surface treatments are inevitable. Corrosion behavior and ICR of AISI 316L specimens coated with 1, 2, and 3 µm thick TiN were investigated. Potentiodynamic (PD), potentiostatic (PS) and electrochemical impedance spectroscopy (EIS) tests were conducted at 80 °C in a pH3 H_2SO_4+2 ppm HF solution purged with either O_2 or H_2 under both simulated cathodic and anodic conditions. The PS corrosion test results revealed that the current densities of the specimens were below 1 µA cm^{-2}. In the simulated cathodic condition, an increase of coating thickness from 1 to 3 µm led to a relatively large decrease of the current density from 0.76 to 0.43 µA cm^{-2}. Furthermore, the ICR values of the coated specimens after the PS test were lower than that of the uncoated specimen before the PS. In general, the TiN coating decreases the ICR, and has enough corrosion resistance in simulated PEMFC conditions. However, none of the coatings achieved the DOE ICR targets.

1. Introduction

There are several critical factors such as separating and distributing fuel and oxidant, carrying away reaction products as well as heat from each cell, which make bipolar plates one of the most significant components in PEMFCs. Therefore, identifying and selecting a proper material to meet mentioned factors is very important. This material, as a bipolar plate, should have high thermal and electrical conductivity, good mechanical and surface properties, adequate corrosion resistance, low interfacial contact resistance (ICR) and gas permeability [1-5]. With regard to the role of the bipolar plates mentioned above, United State

*Corresponding Author's Fax: +983133222446
E-mail address: s.asghari@isrc.ac.ir

Department of Energy (DoE) has determined the quantitative requirements for bipolar plates of fuel cells, as shown in Table 1 [6, 7].

Conventional materials used as bipolar plate materials in PEMFCs are graphite or graphite composite. These materials have excellent chemical stability and corrosion properties, high conductivity, and low ICR. However, the high cost and poor mechanical properties of these materials are the main technical barriers especially for using in transportation application. One of the best strategies to solve these problems is to replace these materials with metallic materials. Metals are good candidates for bipolar plates due to their excellent mechanical strength, high electrical and thermal conductivity, recyclability, low gas permeability, and relatively low material and manufacturing costs. However, the majority of metals do not have sufficient corrosion resistance to be used as bipolar plate material in PEMFCs. The majority of candidate metals such as titanium, niobium, and gold are too expensive. Nevertheless, stainless steels are the most promising materials [8]. It is well known that austenitic stainless steels have better corrosion resistance than the other types of stainless steels such resistant austenitic stainless steels due to its higher Ni content (~10-14 wt%) and the presence of Mo. The AISI 316L grade has a very low carbon content (<0.03 wt%) which is suitable for increasing the weld ability and corrosion resistance [9, 10]. However, corrosion resistance of this type of steel is still not at the desired levels for working in the acidic, humid and warm environment of PEMFCs. Hence, applications of different coating types as CrN, ZrN, conducting polymer, and multilayer coatings on AISI 316L have been studied to improve the corrosion resistance [11-16]. One of the most promising coatings is TiN due to excellent corrosion resistance, high conductivity, a similar water contact angle as graphite, wide industrial feasibility, low cost, and extensive research as well. One of the most widely used methods for TiN coating deposition is Physical Vapor Deposition (PVD).

Cho et al. [17] indicated that the electrical contact resistance and water contact angle of the graphite and TiN-coated 316 were nearly the same. They also reported that the corrosion-protective TiN layer on 316 significantly improved the life length. Their manufactured 1kW short stack operated well

Table 1. DoE technical targets for bipolar plate

Characteristic	Metric	Units	2017	2020
Cost		$ per kW	3	3
Plate H_2 coefficient	ASTM D-134	Std cm^3 (sec cm^2 Pa) @ 80°C, 3 atm 100% RH	<1.3 × 10–^{14}	<1.3 × 10–^{14}
Corrosion, anode[a]	Current density at active peak in potentiodynamic test	μA cm^{-2}	<1	<1 or no active peak
Corrosion, cathode[b]	Current density at +0.6V (Ag/AgCl) in potentiostatic test	μA cm^{-2}	<1	<1
Electrical conductivity	In-plane electrical conductivity (4-pointprobe)	S cm^{-1}	>100	>100
Areal specific resistance[c]	Measured through plane (include both side surfaces)	Ω cm^2	0.02	0.01
Flexural Strength	ASTM-D 790-3	MPa	>25	>25
Forming elongation	ASTM E8M-01	%	40	40

[a] pH 3 0.1 ppm HF, 80°C, potentiodynamic test at 0.1 mVs^{-1}, -0.4V to +0.6V (Ag/AgCl)), de-aerated with Ar purge.

[b] pH 3 0.1 ppm HF, 80°C, potentiostatic test at +0.6V (Ag/AgCl) for >24h, aerated solution.

[c] Includes interfacial contact resistance (on as received and after potentiostatic test) measured both sides per Wang, et al. J. Power Sources 115 (2003) 243-251 at 138 $N.cm^{-2}$.

for 1028 h. Wang et al. [2, 18, 19] investigated the corrosion behavior of PVD TiN-coated AISI 316L and 410 in simulated PEMFC cathode condition. They found that the corrosion of PVD TiN-coated stainless steels was related to the presence of pinholes on the TiN coating surface. Kumagai et al. [20] found that the nano sized TiN as coating on 310 stainless steel bipolar plates can reduce ICR and therefore improve the fuel cell performance. TiN nano particles were not dissolved after 300 h cell operation. Zhang et al. [21] deposited TiN on 304 by means of two surface coating techniques: pulsed bias arc ion plating (PBAIP) and magnetron sputtering (MS). Based on the potentiostatic corrosion tests, TiN-coated 304 corroded in the simulated cathode conditions due to increasing of current density with time. The TiN coating provided lower ICR than the bare 304. The authors stated that the corrosion behavior of TiN-coated 304 depends strongly on microstructures. Dur et al. [22] and Turan et al. [23] have investigated the corrosion and contact resistance of TiN coatings with 0.1, 0.5 and 1 μm coating thicknesses, respectively. Dur et al. [22] reported that some of the PVD TiN-coated AISI 316L samples had lower corrosion resistance than the bare AISI 316L . Turan et al. [23] stated that 1 μm TiN coated samples have the best performance in terms of low ICR; however, ICR increased dramatically after a short term of exposure to corrosion under PEMFC working conditions. Sun et al. [24] have investigated corrosion and contact resistance of TiN coatings with 0.4, and 1 μm coating thicknesses. Their results from potentiostatic test showed that the TiN-coated samples had almost similar behavior as well as higher current density than the bare AISI 316L.

Some of these inconsistent results in the literature may be related to the electrolyte composition, pH and temperature, specimen surface finishing, differences in the material composition and the coating methods [25, 26]. Because of such diverse and sometimes conflicting results in the performance and durability of this type of coating, it seems that further research is needed. Moreover, insufficient works [22-24] on the effect of coating thickness, especially in the thickness range of 1 to 3 μm, on the corrosion behavior of TiN coatings intensifies this need. On the other hand, in most of the studies PD and PS tests have been used to investigate the corrosion behavior of the coating. In spite of having great potential, the Electrical Impedance Spectroscopy (EIS) technique has rarely been used in the studies related to TiN coating. We use this technique in addition to the other techniques (PD and PS) to quantitatively evaluate the corrosion behavior. Also, in most of the previous works [2, 12, 14, 21, 22, 24, 27], the considered time for the PS test to investigate corrosion behavior of specimens has been limited to less than 8 h. In this paper, a longer time (24 h), as recommended by DOE, is considered for the PS tests.

In this work, an attempt is made to investigate the performance and durability of 1 mm-thick AISI 316L metallic bipolar plates coated with TiN in 1, 2, 3 μm thickness using physical vapor deposition (PVD) technique in a simulated PEMFC environment through measuring the corrosion resistance and the ICR. The bare AISI 316L stainless steel (AISI 316L) has been used as a reference material.

2. Materials and Methods

2.1. Test Specimen Preparation

In this study, substrate material was selected from a commercial hot rolled AISI 316L strip with a thickness of 1 mm. The chemical compositions of this strip contained (weight %) 0.027 C, 17.5 Cr, 9.8 Ni, 2.0 Mo, 1.86 Mn, 0.34 Si, 0.4 Cu and 0.004 S. The strip was cut into 25 mm × 25 mm specimens. In order to prepare these specimens for the coating process, they were polished with Sic abrasive paper and alumina powder with 1 μm particle sizes. The polished samples were ultrasonically cleaned in distilled water and mild detergent for 30 min and then dried thoroughly before PVD processing. TiN coating at three different thicknesses (1, 2, and 3 μm) was deposited on AISI 316L substrates by PVD method. TiN coating with thickness below 1μm

is not suitable for applying on bipolar plates [22]. Therefore, the TiN coatings with thicknesses equal and above 1μm are used in this research.

2.2.Coating Thickness Measurements

A metallographic technique was utilized to investigate the accuracy of applied coating thickness. After polishing the cross section of coated samples, they were mounted to produce a plane perpendicular to the coating. Measurements were made on photographs with a scale. Coating thickness was measured at a number of locations along the length of coated samples and the average was computed.

2.3. Corrosion Properties

Among corrosion test methods potentiodynamic (PD), potentiostatic (PS), and electrochemical impedance spectroscopy (EIS) were used for investigating corrosion behavior of both uncoated and coated specimens. In order to simulate the working condition of PEMFC, the temperature, pH, and the composition of electrolyte were selected at 80 °C, 3, and H_2SO_4 + 2 ppm HF, respectively. To simulate the cathode and anode conditions the electrolyte was purged with O_2 and H_2, respectively. A conventional three-electrode system test with a platinum counter electrode, Ag/AgCl electrode bridged with a luggin capillary as reference electrode, and the test specimen as the working electrode were used to conduct the electrochemical experiments using a 2273 Potentiostat (Princeton Applied Research Instruments).

2.3.1. Potentiodynamic (PD) Polarization

PD polarization tests were used to measure and compare corrosion resistances of the uncoated and the coated AISI 316L. The specimens were stabilized for 1 h at the open-circuit potential (OCP). In the PD test, the potential was changed from −150 mV *vs.* OCP to 1 V *vs.* Ag/AgCl at a scan rate of 1 mVs^{-1}. Five specimens were selected for every test and the mean values together with standard deviations of the data were computed.

2.3.2.Potentiostatic (PS) Polarization

PS polarization test was used to investigate the suitability of uncoated and coated AISI 316L as the anode and cathode in a PEMFC. PS tests were conducted for 24 h at the simulated cathode and anode conditions. The simulated anode and cathode conditions were −0.1V *vs.* Ag/AgCl purged with H_2 and 0.6V *vs.* Ag/AgCl purged with O_2, respectively.

2.3.3.Electrochemical Impedance Spectroscopy (EIS)

The EIS measurements were performed at the steady-state in the frequency range of 100 kHz to 0.1 Hz. The AC amplitude was set to 5 mV. Potentiostat/ Galvanostat and Frequency Response Analyzer PARSTAT 2273 were used for the EIS measurements. In order to obtain the stationary conditions necessary for impedance measurements, the working electrodes were polarized for 24 h at the simulated cathode and anode conditions. The simulated cathode and anode conditions were −0.1V *vs*. Ag/AgCl purged with H_2 and 0.6V *vs*.Ag/AgCl purged with O_2, respectively. For every test, five specimens were selected and the mean values and the standard deviations of data were computed. EIS spectra were interpreted using the ZView software and modified complex nonlinear least square (CNLS) fitting method [28].

2.4. Interfacial Contact Resistance (ICR)

Wang's method [29] was used to measure the ICR of uncoated and TiN coated AISI 316L specimens and a graphite specimen for comparison purposes. As shown in Fig. 1(a), the specimens were sandwiched between two pieces of gas diffusion layer (GDL):(SIGRACET® 34 BC) and two Au coated copper plates.

In order to calculate the total resistance of this setup by Ohm law ($R=VI^{-1}$), an electrical current (1 A) was applied via the two Au coated copper plates and

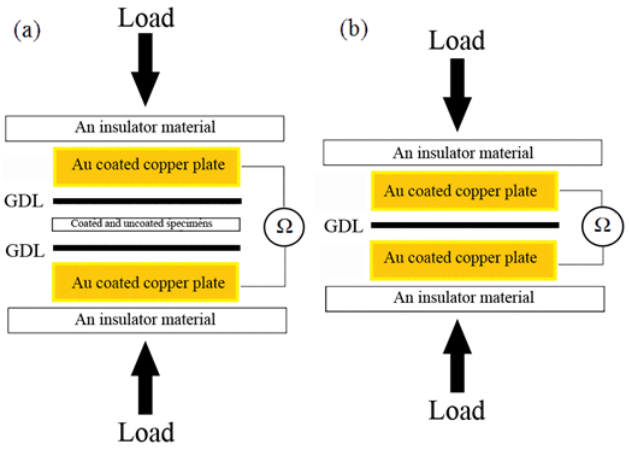

Fig. 1. Schematic for measuring interfacial contact resistance (a) specimen sandwiched between two pieces of GDL and two Au coated copper plates, (b) GDL sandwiched between two Au coated copper plates.

then the total voltage drop through this setup was measured as a function of the gradually increasing compaction force. The total resistance of this setup (R_{T1}) consists of bulk resistance of two Au coated copper plates ($2R_{CP}$), two ICRs between the Au coated copper plate and GDL ($2R_{CP|GDL}$), two bulk resistances of GDL ($2R_{GDL}$), two ICRs between the GDL and the specimen ($2R_{GDL|S}$), and the bulk resistance of the specimen (R_S).The R_{T1} can be expressed as:

$$R_{T1}=2R_{CP}+2R_{CP|GDL}+2R_{GDL}+2R_{GDL|S}+R_S \quad (1)$$

$R_{CP|GDL}$ can be calculated by using an arrangement shown in Fig. 1(b).

This configuration consists of the bulk resistance of two Au coated copper plates (R_{CP}) and two interfacial contact resistances between Au coated copper plate and GDL ($2R_{CP|GDL}$), and the bulk resistance of the GDL (R_{GDL}). Therefore, R_{T2} can be expressed as:

$$R_{T2} = 2R_{CP} + 2R_{CP|GDL} + R_{GDL} \quad (2)$$

The ICR between the specimen and the GDL can be calculated by using (1) and (2) equations as follows:

$$R_{GDL|S} = 0.5 \times (R_{T1} - R_{T2} - R_{GDL} - R_S) \quad (3)$$

Bulk resistance values of the GDL and the specimen are very small (compared with the other resistances) and negligible [14, 30, 31]. Hence, the ICR between the GDL and the specimen can be expressed as follows:

$$R_{GDL|S} \approx 0.5 \times (R_{T1} - R_{T2}) \quad (4)$$

Double sided compaction with a pressure in the range of 25 to 310N.cm^{-2} was applied on specimens with a contact area of 2.25 cm^2 (Press: SMT 20, SANTAM Co.) with the speed of 0.1 mm min^{-1}. Before measurement of the ICR, bare AISI 316L specimens were polished with #600 grit SiC abrasive paper. Then, uncoated and TiN coated specimens were cleaned with acetone and dried with nitrogen. For each measurement test, GDL was only used once.

3. Results and Discussions

3.1. Potentiodynamic (PD) Corrosion Test

Corrosion potential and current can be obtained from the potentiodynamic (PD) polarization curve. These parameters indicate the corrosion resistance of the materials. A lower corrosion current and higher corrosion potential generally show a higher corrosion resistance. Fig. 2 shows PD curves of the bare specimen and the TiN coated specimens with three different thicknesses (1, 2, and 3 μm) in both the simulated cathode (purged with O_2, Fig. 2(a)) and anode conditions (purged with H_2, Fig. 2(b)). Table 2 shows corrosion properties of the uncoated and coated specimens, such as corrosion potential (E_{corr}) and corrosion current density (i_{corr}), obtained from a Tafel plot by extrapolating the linear portion of the curve to E_{CORR}, as shown in Fig. 3.

As can be seen, in the simulated cathode conditions the corrosion potential of the bare AISI 316L is lower than those of the coated specimens. Thus, the applied TiN coating on a AISI 316L substrate retards the corrosion. From Fig. 2(a) and Table 2, we can see that the corrosion behavior of the coated specimens with three different thicknesses are almost the same. Corrosion current densities (icorr) of all coated

Table 2. Corrosion properties of uncoated and TiN-coated AISI 316L specimens in a pH3 H_2SO_4+2 ppm HF solution at 80 °C with either H_2 or O_2 purging obtained from potentiodynamic polarization curve where the potential reference was Ag/AgCl

	Purge Gas	E_{corr}(mV)	i_{corr} (μA cm^{-2})	P_i(%)
AISI 316L	H_2	-13±14	0.099±0.011	-
	O_2	12±9	0.176±0.031	-
1 μm TiN	H_2	191±11	0.077±0.027	22.22
	O_2	226±16	0.076±0.017	56.82
2 μm TiN	H_2	219±18	0.062±0.021	37.37
	O_2	209±14	0.071±0.024	59.66
3 μm TiN	H_2	195±12	0.042±0.027	57.58
	O_2	258±21	0.066±0.014	62.5

specimens are below 1 μA cm^{-2} and in the range of 0.066 to 0.076 μA cm^{-2}; while the corrosion current density (icorr) of the bare specimen is 0.176 μAc m^{-2}. Thus TiN coating in the simulated cathode condition increases the corrosion resistance.

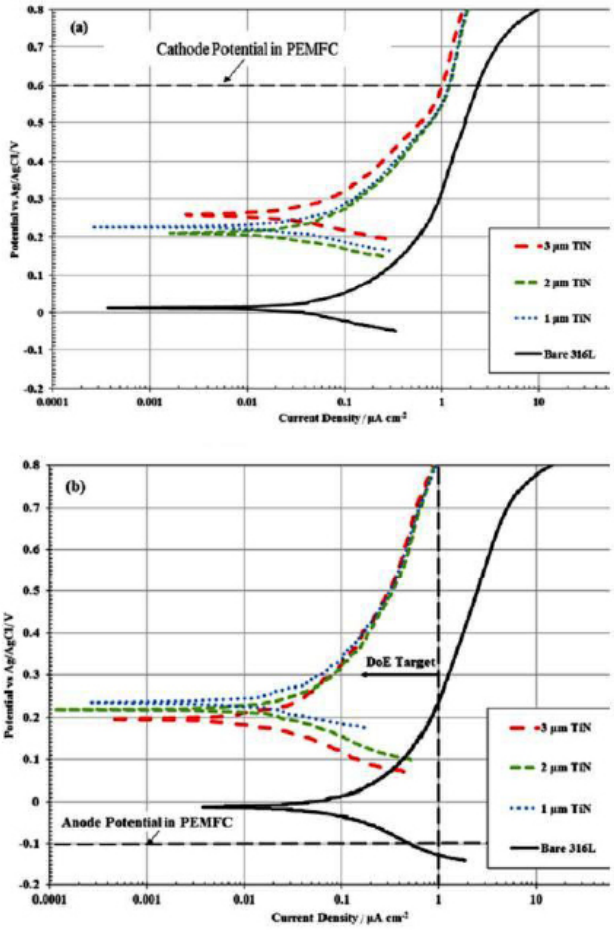

Fig. 2. Potentiodynamic polarization curves for uncoated and TiN-coated specimens in a pH3 H_2SO_4+2 ppm HF solution at 80 °C with (a) O_2 purging and (b) H_2 purging.

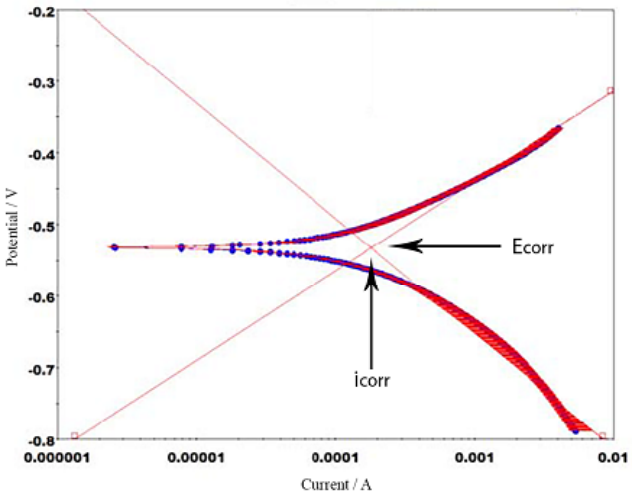

Fig. 3. Corrosion potential (E_{corr}) and current density (i_{corr}) obtained from a Tafel plot by extrapolating the linear portion of the curve to E_{CORR}.

According to Fig. 2(b) and Table 2, in the simulated anode conditions the icorr of all coated specimens is below 1 μAcm^{-2} and is located in the range of 0.042 to 0.077 μA cm^{-2}. Furthermore, the i_{corr} of the bare specimen is 0.099 μAcm^{-2}. According to Fig. 2(b(the uncoated and the TiN-coated specimens do not exhibit any active peak which is in agreement with DOE requirements. In both cathode and anode conditions, the coated specimens display much better corrosion resistance than the bare specimen.

The protective efficiency (P_i) of the coating layer is calculated using the following equation [12]:

$$P_i(\%) = 100 \times (1 - (\frac{i_{corr}}{i^0_{corr}})) \quad (5)$$

Where i_{corr} and i^0_{corr} are the corrosion current densities

in the presence and absence of the coating on AISI 316L, respectively. Table 2 shows that the protective efficiency increases as the coating thickness increases. In both cathode and anode conditions, 3µm-thick-TiN coated specimen has the highest protective efficiency.

3.2 Potentiostatic (PS) Corrosion Test

Figs. 4(a) and 4(b) show the potentiostatic polarization curves at +0.6V *vs*. Ag, AgCl electrode in an O_2-purged solution and−0.1V *vs*. Ag, AgCl electrode in a H_2-purged solution.

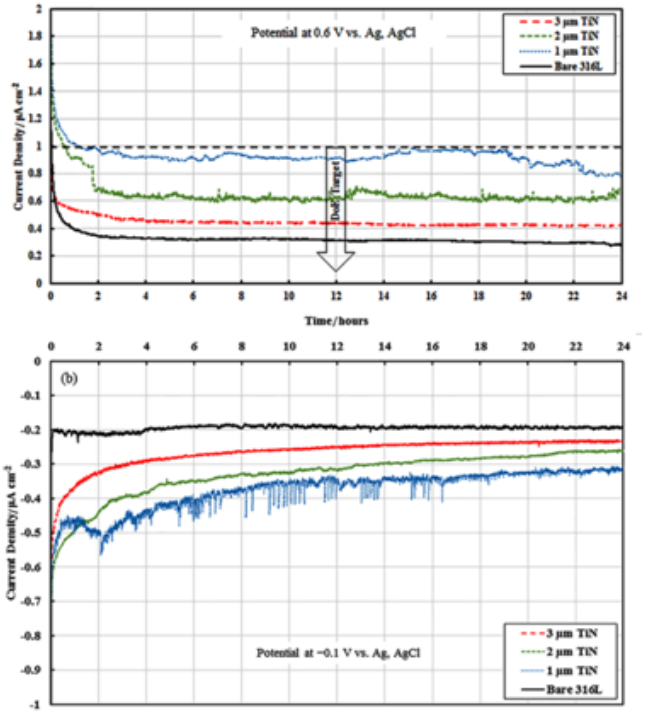

Fig. 4. Potentiostatic polarization curves for uncoated and TiN-coated specimens in a pH3 H_2SO_4+2 ppm HF solution at 80 °C with (a) O_2 purging and (b) H_2 purging.

In most of the previous works [2, 12, 14, 21, 22, 24, 27], the considered time for the PS test to investigate corrosion behavior of specimens was short and less than 8 h. This can cause diverse and sometimes conflicting results. In this paper, a longer time (24 h), in agreement with DOE requirements, is considered for the PS tests. The current density values of the coated and uncoated specimens in both simulated cathode and anode conditions after 24 h are listed in Table 3. In the simulated cathode conditions (Fig. 4(a) and Table 3), the bare specimen shows lower current density values than the coated specimens after 24 h. This result is in agreement with many previous works [2, 14, 22, 24]. The rapid decrease of current density at the beginning of the PS test is related to the formation of passive layers. The results also show that the current densities of the uncoated and the coated specimens decrease as time increases. Thus, it can be concluded that the passive layers formed on the specimen surfaces in the simulated cathode conditions are stable and can protect the sub layers from corrosion. By increasing the thickness from 1 to 3 µm, the current density decreases from 0.76 to 0.43 µA cm^{-2}. Thus the corrosion resistance increases as the coating thickness increases. The current densities of both uncoated and coated specimens are below 1 µA cm^{-2} which is in agreement with the DOE target.

In the simulated anode conditions (Fig. 4(b) and Table 3), the corrosion current density of the uncoated specimen stabilizes at about -0.2 µA cm^{-2}. The corrosion current densities of coated specimens decrease as time increases. The corrosion current densities of both uncoated and coated specimens are negative. This negative current provides cathodic protection for both the uncoated and coated specimens. Therefore, the coated specimens undergo no corrosion in the simulated anodic conditions.

3.3.Electrochemical Impedance Spectroscopy (EIS)

Nyquist plots measured at the simulated cathodic and anodic conditions are shown in Fig. 5(a) and (b), respectively.

Table 3.The current density for TiN coated specimens and bare specimen in both simulated cathode and anode conditions after 24h

The stabilized current density value	Bare AISI 316L (µA cm^{-2})	1 µm TiN (µA cm^{-2})	2 µm TiN (µA cm^{-2})	3 µm TiN (µA cm^{-2})
simulated cathode condition after 24h	0.27	0.76	0.69	0.43
simulated anode condition after 24h	-0.20	-0.31	-0.26	-0.23

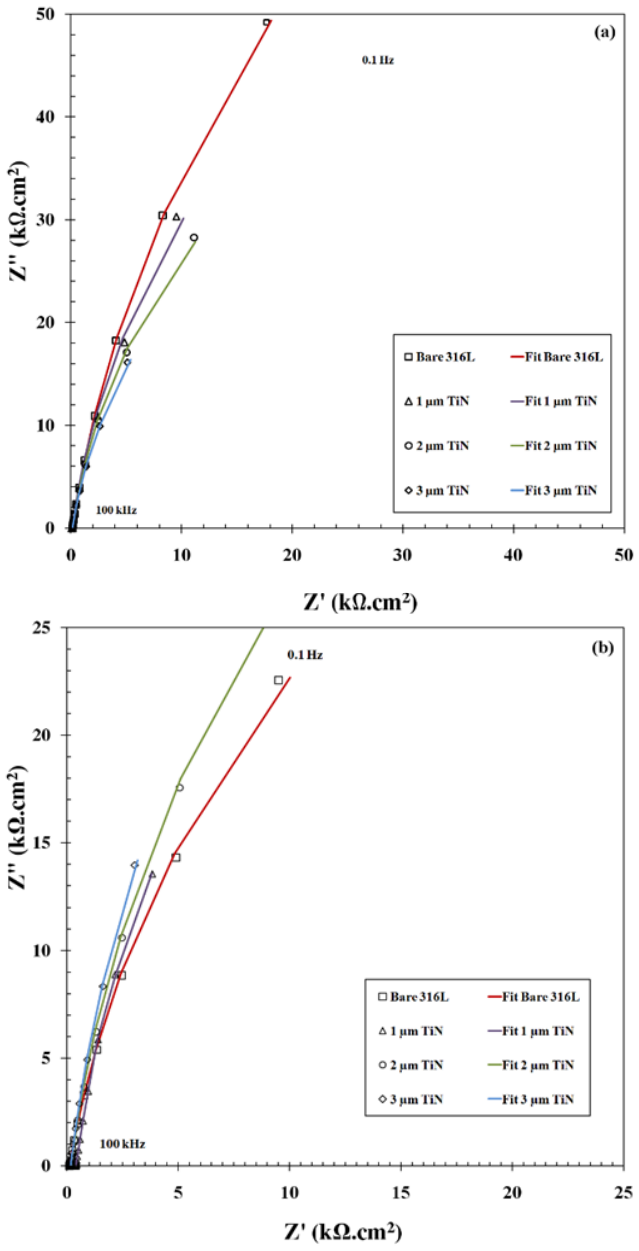

Fig. 5. Nyquist plots of uncoated and TiN-coated specimens on steel (a) in the simulated cathode environments, and (b) in the simulated anode environments.

In general, one semi-circle and two semi-circles with a depressed angle are found for the bare and the coated specimens over the explored frequency range [32]. The experimental data in the figures are presented as points and the continuous lines are obtained by curve fitting [33]. A depressed semi-circle in the complex–plane plots suggests that the inhomogeneity exists on the electrode surface. This phenomenon can theoretically be modeled with a constant phase element (CPE), which replaces the capacitance of the double layer (C_{dl}) [32-34]. The presence of the CPE causes a rotation of the complex–plane plot clockwise by a constant angle. The constant phase element impedance is described by:

$$Z_{CPE} = C^{-1}(j\omega)^{-(1-\alpha)} \quad (6)$$

where ω is the angular frequency of the AC voltage, $j=\sqrt{(-1)}$, α the frequency independent parameter related to the depression angle φ which is equal to α×90◦ and C is a constant related to the double-layer capacitance of the electrodes, C_{dl}.

Fig.6 shows the equivalent circuits used for fitting the EIS data of the bare specimen.

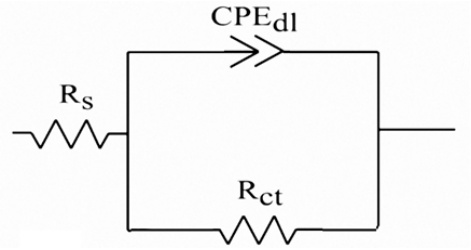

Fig. 6. Electrochemical equivalent circuits used for fitting the experimental data of the bare AISI 316L R_s: solution resistance, R_{ct}: Faradic process resistance, and CPE_{dl}: constant phase element of double layer.

One constant phase element (one CPE) model (Fig.6) was used to fit the EIS data [35-37]. The one CPE model (Fig. 6) consists of solution resistance (R_s), being in series with a parallel combination of the Faradic process resistance (R_{ct}), and constant phase element of the double layer (CPE_{dl}).

EIS fitted data represent corrosion resistance, R_{corr}, and C_{dl} of the specimens. The C_{dl} term is related to the porosities of the specimens [38-40], and R_{corr} is used as a measure of the barrier properties of the specimens. R_{corr} is the summation of the pore resistance (R_p) and charge transfer resistance (R_{ct}):

$$R_{corr} = R_p + R_{ct} \quad (7)$$

It has been recognized that high values of R_{ct} and low values of C_{dl} imply a better corrosion protective

ability of coatings [41-45]. The R_{ct} and C_{dl} values of TiN coated specimens are shown in Table 4. The R_{ct} and C_{dl} values rise as coating thickness increases. Thus, the 3µm-TiN coated specimen has a slightly higher value of R_{corr} than the other ones in the simulated anode and cathode environments.

As a result, it can be concluded that TiN coated specimens were in a passive state in the simulated conditions, and TiN coated specimens have acceptable R_{corr} values in the simulated environments. Additionally, a comparison of C_{dl} values measured by impedance of specimens indicates that C_{dl} increases as TiN coating thickness increases. This can stem from the presence of open pores and the degree of heterogeneity of the surface associated with increasing the coating thickness during the PVD process.

3.4. Interfacial Contact Resistance (ICR)

As discussed in the materials and methods section, the bulk resistance values are negligible compared to the ICR values. Although the coating thickness cannot directly affect the ICR values of the coated specimens, it indirectly affects this value by changing morphology and surface properties. The ICR between the GDL and the specimens (bare AISI 316L, and 3µm-thick-TiN coated AISI 316L) at different compaction pressures, before and after the PS test in the anode simulated condition, was measured for both sides. The ICR of a typical graphite plate was also measured for comparison. The ICR results are presented in Fig. 7. The inset in Fig. 7 is an enlarged plot at compaction pressures in the range of 100–320N.cm^{-2}.

In general, the ICR decreases rapidly at low compaction pressure range and then declines gradually at higher compaction pressures. In a specified compaction pressure, the resistance increases in the order of Graphite <TiN<TiN after PS < 316L < 316L after PS.

The typical range of the assembly pressure in a PEM

Table 4. Corrosion resistance, R_{corr}, double layer capacity, C_{dl}, in the simulated cathode and anode environments

	Simulated cathode environments		Simulated anode environments	
Electrode	C_{dl} (µF cm^{-2})	R_{corr} (Ω cm^2)	C_{dl} (µF cm^{-2})	R_{corr} (Ω cm^2)
AISI 316L	27.6	(3.39±0.54)×10^{+05}	56.9	(2.8±0.64)×10^{+05}
1 µm TiN	46.2	(3.67±1.29)×10^{+05}	69.1	(8.25±0.81)×10^{+05}
2 µm TiN	48.0	(5.18±0.72)×10^{+05}	93.7	(8.43±0.49)×10^{+05}
3 µm TiN	85.4	(8.53±0.83)×10^{+05}	117.2	(8.58±0.63)×10^{+05}

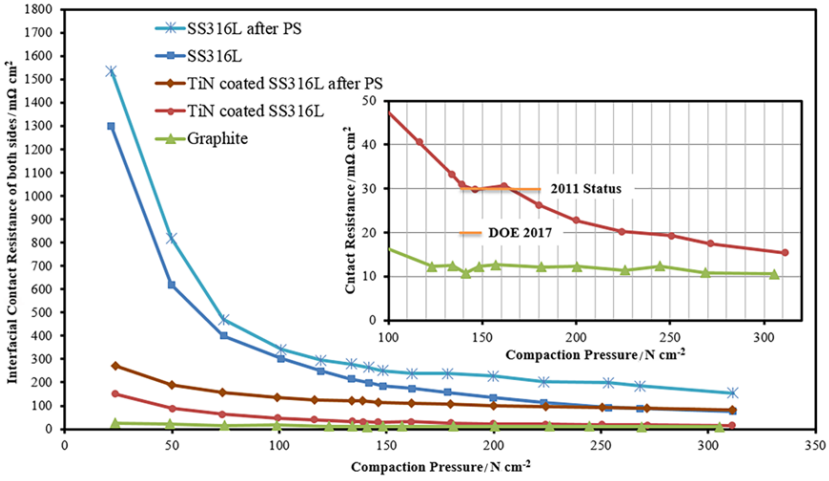

Fig. 7. Interfacial Contact Resistance of graphite, bare AISI 316L, and 3µm-thick-TiN coated specimens before and after PS test measured both sides.

fuel cell is about 100~150N.cm^{-2}. The compaction pressure of 120~140N.cm^{-2} was used in the single cells and stacks in this work. A compaction pressure of 138 N.cm^{-2} for the comparison of the ICR of different coated and uncoated samples was used as the reference pressure and is also used in the DOE technical target. At a compaction pressure of 138 N.cm^{-2}, the ICR values of graphite, coated specimens before and after PS and uncoated specimens before and after PS are 10.8, 29.5, 122, 199.2 and 265 mΩ cm^2, respectively. It seems that the passive layer formation on the surface of the uncoated and the coated specimens after the PS test leads to an increase of ICR values. Although the passive layer formation has increased the ICR value of the coated specimen after the PS test, this value is still lower than that of uncoated specimen before the PS. Hence, it seems that the formed passive layer on the surface of the coated specimen leads to a better conductivity than the passive layer on the surface of the uncoated specimens before and after the PS. The higher ICR of bare AISI 316L than that of TiN coated specimen may be related to the natural oxide passive layer formed on the stainless steel surface [14, 22].

4. Conclusions

The performance and durability of 1 mm-thick AISI 316L metallic bipolar plates TiN coated with three different thicknesses (1, 2, and 3 μm) using a physical vapor deposition (PVD) technology is investigated in a simulated PEMFC environment by measuring the corrosion resistance and the ICR.

The results from the potentiodynamic polarization curves in both simulated cathode and anode conditions showed that as the TiN coating thickness increased the protective efficiency was augmented. In the simulated cathode conditions potentiostatic test results elucidated that the passive layers formed on the specimen surfaces are stable and can protect the sub layers from corrosion, since the current densities of the uncoated and the TiN coated specimens decrease as the time increased. The current densities decrease from 0.76 to 0.43 μA cm^{-2} as the TiN thickness increases from 1 to 3 μm. This relatively large reduction of the current density leads to the increase of corrosion resistance. In the simulated anode conditions, the uncoated and the TiN-coated specimens undergo no corrosion because the corrosion current densities of both the uncoated and the TiN-coated specimens are negative, and this negative current provides cathodic protection. The EIS results showed that the TiN coated specimens have high value of R_{corr} which indicate that the coated specimens were in passive state in the simulated environments.

From the PD test in the simulated anode conditions, the uncoated and TiN-coated specimens do not exhibit any active peak. From the PS test in the simulated cathode conditions, the current densities of both uncoated and TiN coated specimens were below 1 μAcm^{-2} and in agreement with the DOE target.

The ICR values at a specified compaction pressure increase by the order of Graphite <TiN<TiN after PS < 316L < 316L after the PS test. Thus, it can be concluded that the formed passive layer on the surface of the coated specimen caused better conductivity than the passive layer on the surface of the uncoated specimens before and after the PS test. TiN coating cannot meet the DOE target but it can strongly decrease the ICR value.

Eventually, the ICR value of bare AISI 316L becomes too high to be used without a coating in PEMFC. The TiN coating decreases the ICR and has high enough corrosion resistance in simulated aggressive PEMFC environments.

Acknowledgment

The authors would like to thank the financial support of Renewable Energy Organization of Iran (SUNA) and Mr. Faghih Imani from Institute of Materials and Energy who provided insight and expertise that greatly assisted this research.

7. References

[1] Wilkinson D.P., Zhang J., Hui R., Fergus J., Li X., "Proton exchange membrane fuel cells : materials properties and performance", first ed., CRC Press/Taylor & Francis, Boca Raton, FL, 2010, 55: 225.

[2] Wang Y., Northwood D.O., "An investigation into TiN-coated 316L stainless steel as a bipolar plate material for PEM fuel cells", J. Power Sources, 2007, 165: 293.

[3] Yoon W., Huang X., Fazzino P., Reifsnider K.L., Akkaoui M.A., "Evaluation of coated metallic bipolar plates for polymer electrolyte membrane fuel cells", J. Power Sources, 2008, 179: 265.

[4] Hermann A., Chaudhuri T., Spagnol P., "Bipolar plates for PEM fuel cells: A review", Int. J. Hydrogen Energy, 2005, 30: 1297.

[5] Asghari S., Mokmeli A., Samavati M., "Study of PEM fuel cell performance by electrochemical impedance spectroscopy", Int. J. Hydrogen Energy, 2010, 35: 9283.

[6] Fuel Cell Technical Team Roadmap, U.S. DRIVE (Driving Research and Innovation for Vehicle efficiency and Energy sustainability), 2013, pp. 9.

[7] DeCuollo G., "Low Cost PEM Fuel Cell Metal Bipolar Plates", Technoport 2012, 1: 13.

[8] Steele B.C.H., Heinzel A., "Materials for fuel-cell technologies", Natur, 2001, 414: 345.

[9] Jones D.A., 2nd ed. Principles and prevention of corrosion, Prentice Hall, New Jersey, 1996.

[10] Atkinson J., VanDroffelaar H., "Corrosion and its Control", 1982, 1: 55.

[11] Nam N.D., Kim J.-G., "Electrochemical behavior of CrN coated on 316L stainless steel in simulated cathodic environment of proton exchange membrane fuel cell", JaJAP, 2008, 47: 6887.

[12] Lee S.H., Kakati N., Maiti J., Jee S.H., Kalita D.J., Yoon Y.S., "Corrosion and electrical properties of CrN- and TiN-coated 316L stainless steel used as bipolar plates for polymer electrolyte membrane fuel cells", Thin Solid Films, 2013, 529: 374.

[13] Barranco J., Barreras F., Lozano A., Maza M., "Influence of CrN-coating thickness on the corrosion resistance behaviour of aluminium-based bipolar plates", J. Power Sources, 2011, 196: 4283.

[14] Wang L., Northwood D.O., Nie X., Housden J., Spain E., Leyland A., Matthews A., "Corrosion properties and contact resistance of TiN, TiAlN and CrN coatings in simulated proton exchange membrane fuel cell environments", J. Power Sources, 2010, 195: 3814.

[15] Joseph S., McClure J.C., Chianelli R., Pich P., Sebastian P.J., "Conducting polymer-coated stainless steel bipolar plates for proton exchange membrane fuel cells (PEMFC)", Int. J. Hydrogen Energy, 2005, 30: 1339.

[16] Lee Y.-B., Lim D.-S., "Electrical and corrosion properties of stainless steel bipolar plates coated with a conduction polymer composite", CAP, 2010, 10: S18.

[17] Cho E., Jeon U.S., Hong S.A., Oh I.H., Kang S.G., "Performance of a 1 kW-class PEMFC stack using TiN-coated 316 stainless steel bipolar plates", J. Power Sources, 2005, 142: 177.

[18] Wang Y., Northwood D.O., "An investigation of the electrochemical properties of PVD TiN-coated SS410 in simulated PEM fuel cell environments", Int. J. Hydrogen Energy, 2007, 32: 895.

[19] Wang Y., Northwood D.O., "Effect of substrate material on the corrosion of TiN-coated stainless steels in simulated anode and cathode environments of proton exchange membrane fuel cells", J. Power Sources, 2009, 191: 483.

[20] Kumagai M., Myung S.T., Asaishi R., Sun Y.K., Yashiro H., "Nanosized TiN-SBR hybrid coating of

stainless steel as bipolar plates for polymer electrolyte membrane fuel cells", Electrochim. Acta, 2008, 54: 574.

[21] Zhang D., Duan L., Guo L., Tuan W.H., "Corrosion behavior of TiN-coated stainless steel as bipolar plate for proton exchange membrane fuel cell", Int. J. Hydrogen Energy, 2010, 35: 3721.

[22] Dur E., Cora Ö.N., Koç M., "Experimental investigations on the corrosion resistance characteristics of coated metallic bipolar plates for PEMFC", Int. J. Hydrogen Energy, 2011, 7162.

[23] Turan C., in: MecEn, Virginia Commonwealth University, Richmond, Virginia, US, 2011, pp. 198.

[24] Sun H., Cooke K., Eitzinger G., Hamilton P., Pollet B., "Development of PVD coatings for PEMFC metallic bipolar plates", Thin Solid Films, 2013, 528: 199.

[25] Antunes R.A., Oliveira M.C.L., Ett G., Ett V., "Corrosion of metal bipolar plates for PEM fuel cells: A review", Int. J. Hydrogen Energy, 2010, 35: 3632.

[26] Wang H., Turner J., "Reviewing metallic PEMFC bipolar plates", Fuel Cells, 2010, 10: 510.

[27] Tian R., Sun J., "Corrosion resistance and interfacial contact resistance of TiN coated 316L bipolar plates for proton exchange membrane fuel cell", Int. J. Hydrogen Energy, 2011, 36: 6788.

[28] Li M., Luo S., Zeng C., Shen J., Lin H., Cao C.n., "Corrosion behavior of TiN coated type 316 stainless steel in simulated PEMFC environments", Corros. Sci., 2004, 46: 1369.

[29] Wang H., Sweikart M.A., Turner J.A., "Stainless steel as bipolar plate material for polymer electrolyte membrane fuel cells", J. Power Sources, 2003, 115: 243.

[30] André J., Antoni L., Petit J.-P., De Vito E., Montani A., "Electrical contact resistance between stainless steel bipolar plate and carbon felt in PEFC: A comprehensive study", Int. J. Hydrogen Energy, 2009, 34: 3125.

[31] Jayaraj J., Kim Y.C., Seok H.K., Kim K.B., Fleury E., "Development of metallic glasses for bipolar plate application", Materials Science and Engineering: A, 2007, 449: 30.

[32] Ekdunge P., Jüttner K., Kreysa G., Kessler T., Ebert M., Lorenz W., "Electrochemical impedance study on the kinetics of hydrogen evolution at amorphous metals in alkaline solution", J. Electrochem. Soc., 1991, 138: 2660.

[33] Macdonald J.R., Johnson W.B., "Fundamentals of Impedance Spectroscopy", Impedance Spectroscopy, 2005, 1: 44.

[34] Nyikos L., Pajkossy T., "Fractal dimension and fractional power frequency-dependent impedance of blocking electrodes", Electrochim. Acta, 1985, 30: 1533.

[35] Chen L., Lasia A., "Ni-Al Powder Electrocatalyst for Hydrogen Evolution", J. Electrochem. Soc., 1993, 140: 2464.

[36] Los P., Lasia A., Ménard H., Brossard L., "Impedance studies of porous lanthanum-phosphate-bonded nickel electrodes in concentrated sodium hydroxide solution", J. Electroanal. Chem., 1993, 360: 101.

[37]Jurczakowski R., Hitz C., Lasia A., "Impedance of porous gold electrodes in the presence of electroactive species", J. Electroanal. Chem., 2005, 582: 85.

[38] La Mantia F., Vetter J., Novák P., "Impedance spectroscopy on porous materials: A general model and application to graphite electrodes of lithium-ion batteries", Electrochim. Acta, 2008, 53: 4109.

[39] Liu X., Xiong J., Lv Y., Zuo Y., "Study on corrosion electrochemical behavior of several different coating systems by EIS", Prog. Org. Coat., 2009, 64: 497.

[40] Jüttner K., "Electrochemical impedance spectroscopy (EIS) of corrosion processes on inhomogeneous surfaces",

Electrochim. Acta, 1990, 35: 1501

[41] Brown R., Alias M.N., Fontana R., "Effect of composition and thickness on corrosion behavior of TiN and ZrN thin films", Surf. Coat. Technol., 1993, 62: 467.

[42] Huang J.-H., Ouyang F.-Y., Yu G.-P., "Effect of film thickness and Ti interlayer on the structure and properties of nanocrystalline TiN thin films on AISI D2 steel", Surf. Coat. Technol., 2007, 201: 7043.

[43] Yao Z., Jiang Z., Wang F., "Study on corrosion resistance and roughness of micro-plasma oxidation ceramic coatings on Ti alloy by EIS technique", Electrochim. Acta, 2007, 52: 4539.

[44] Gilbert J.L., Electrochemical Behavior of Metals in the Biological Milieu, Elsevier, Oxford, 2011.

[45] Chen Q., McEwen G.D., Zaveri N., Karpagavalli R., Zhou A., Chapter 9 - Corrosion Resistance of Ti6Al4V with Nanostructured TiO_2 Coatings, in: Emerging Nanotechnologies in Dentistry, William Andrew Publishing, Boston, 2012, pp. 137.